JOURNAL OF NEUROTRAUMA XX:1–11 (Month XX, 2017)

DOI: 10.1089/neu.2016.4701

Original Article

The Alternative Receptor for Complement Component 5a, C5aR2, Conveys Neuroprotection in Traumatic Spinal Cord Injury

Patrick J.C. Biggins,[1] Faith H. Brennan,[1] Stephen M. Taylor,[1] Trent M. Woodruff,[1] and Marc J. Ruitenberg[1–3]

Abstract

This study investigated the role of the alternative receptor for complement activation fragment C5a, C5aR2, in secondary inflammatory pathology after contusive spinal cord injury (SCI) in mice. *C5ar2*$^{-/-}$ mice exhibited decreased intraparenchymal tumor necrosis factor alpha and interleukin-6 acutely post-injury, but these reductions did not translate into improved outcomes. We show that loss of C5aR2 leads to increased lesion volumes, reduced myelin sparing, and significantly worsened recovery from SCI in *C5ar2*$^{-/-}$ animals compared to wild-type (WT) controls. Loss of C5aR2 did not alter leukocyte mobilization from the bone marrow in response to SCI, and neutrophil recruitment/presence at the lesion site was also not different between genotypes. Acute treatment of SCI mice with the selective C5aR1 antagonist, PMX205, improved SCI outcomes, compared to vehicle controls, and, importantly, fully alleviated the worsened recovery of *C5ar2*$^{-/-}$ mice compared to their WT counterparts. Collectively, these findings indicate that C5aR2 is neuroprotective and a novel target to restrain injurious C5a signaling after a major neurotraumatic event.

Keywords: degeneration; inflammation; neural injury; secondary insult; traumatic spinal cord injury

Introduction

Complement system activation is one of the earliest acting aspects of the inflammatory response to spinal cord injury (SCI) and represents a principal source of secondary damage.[1–3] Complement activation is zymogenic, with proteolytic cleavage of complement precursors occurring in response to microhemorrhaging and/or upon encountering cellular debris.[4] Proteolytic activation of the central complement component 5 (C5) leads to generation of the anaphylatoxin, C5a, a small glycoprotein (74 amino acids, ~11 kDa) with well-established, potent, proinflammatory actions.[5] In addition, complement activation and associated C5a signaling has also been directly linked to neurotoxicity and neuronal apoptosis,[6–10] although, somewhat paradoxically, a protective role against excitoxicity has also been reported.[11–13]

C5a exerts its biological effects through interaction with two known receptors: the G-protein-coupled C5a receptor 1 (C5aR1) and a second receptor, C5aR2 (C5L2), which interacts with β-arrestin[14] but does not bind G protein.[15] Activation of the C5a–C5aR1 axis in response to acquired central nervous system (CNS) injury is well established and mostly considered injurious, at least acutely, in models of intracerebral hemorrhage,[16] ischemic stroke,[17] traumatic brain injury (TBI),[18] and SCI.[3,19,20]

Whereas the actions of C5aR1 in acquired CNS injury are reasonably well characterized, the role of the alternative C5a receptor, C5aR2, is much less understood. Previous studies with human neutrophils, one of the earliest infiltrating peripheral immune cells in SCI, have indicated that C5aR2 negatively regulates C5aR1 signaling and chemotaxis through its interaction with β-arrestin 2.[14] A similar interaction between C5aR2 and β-arrestins has been reported in human monocyte-derived macrophages.[21] Direct activation of C5aR2 with selective ligands was also recently shown to inhibit C5aR1-mediated signaling and interleukin-6 (IL-6) secretion from human monocyte-derived macrophages and to ameliorate C5a-induced neutrophil mobilization *in vivo*.[22] Further, C5aR2 stimulation blocks NLR family pyrin domain-containing 3 inflammasome assembly in activated human CD4^{+} T cells, leading to blunted T_H1 responses.[23] Given the established roles of neutrophils, macrophages, and C5a signaling in secondary immune-mediated pathology during the acute phase of SCI,[3,19,24–27] we hypothesized that C5aR2 may act as a negative regulator of the (neuro-) inflammatory response to SCI. In the present study, we therefore

[1]School of Biomedical Sciences, The University of Queensland, Brisbane, Australia.
[2]Queensland Brain Institute, The University of Queensland, Brisbane, Australia.
[3]Trauma, Critical Care and Recovery, Brisbane Diamantina Health Partners, Brisbane, Australia.

used C5aR2 knockout mice[28] to directly probe the function of this C5a receptor in relation to SCI outcomes. We also combined this with pharmacological inhibition of C5aR1 in order to understand the interplay between these two C5a receptors after a major neurotraumatic event.

Methods

Animals

A total of 80 adult female C57BL6/J wild-type (WT) and 52 age-matched C5aR2 knockout (hereafter referred to as *C5ar2*$^{-/-}$) mice were used in this study; *C5ar2*$^{-/-}$ mice were backcrossed for more than 10 generations onto a C57BL6/J genetic background. All experimental mice were obtained from breeding colonies at The University of Queensland Biological Resources facility (Brisbane, Australia) (*C5ar2*$^{-/-}$ and C57BL6/J). Animals were housed on a 12-h light-dark cycle in individually ventilated cages, with *ad libitum* access to food and water. All experimental procedures were approved by The University of Queensland's Animal Ethics Committee (Anatomical Biosciences) and conducted in accord with both the Australian code for the care and use of animals for scientific purposes, and the ARRIVE guidelines.[29]

Surgical procedures and post-operative care

Mice were anaesthetized by intraperitoneal (i.p.) injection with xylazine (10 mg/kg; Ilium; Troy Laboratories, Glendenning, Australia) and zolazepam (50 mg/kg; Virbac Laboratories, Carros, France) and subjected to a severe contusive SCI as detailed previously.[30] In brief, the ninth thoracic (T9) target vertebra was identified based on anatomical landmarks,[31] followed by removal of the dorsal arch (i.e., laminectomy) to expose the spinal cord. A force-controlled 70-kilodyne (kDyne) impact was then applied (spinal level T10/T11) with the Infinite Horizon Impactor (Precision Systems and Instrumentation, Lexington, KY). After impact, the surgery site was rinsed with sterile saline and the paravertebral muscles sutured using 5-0 Coated Vicryl (Polyglactin 910) sutures (Ethicon Endo-Surgery, Inc., Cincinnati, OH), after which the skin was closed using MiChel wound clips (KLS Martin Group, Jacksonville, FL). Post-operative care involved subcutaneous administration of a single dose of buprenorphine (0.05 mg/kg) in Hartmann's sodium lactate solution for analgesia and a prophylactic dose of gentamicin (1.0 mg/kg, Ilium) for 5 days post-surgery. Bladders were checked and, where necessary, voided manually twice-daily until the experimental endpoint.

Order of surgery (genotype and/or pharmacological treatment group, where appropriate) was randomized based on predetermined lists. The experimenter conducting the surgery was blinded to genotype and/or treatment groups throughout all aspects of surgery. SCI mice, reidentifiable based on tail marks, were then randomly allocated to cages, each labeled with a code tag for that particular experimental group (e.g., group A, B, C, etc.); 3–4 mice were housed per box for the duration of the experiment.

Actual applied force parameters and associated tissue displacements for the various WT and *C5ar2*$^{-/-}$ experimental cohorts are detailed in Supplementary Tables 1 and 2 (see online supplementary material at http://www.liebertpub.com). Only animals with a deviation $<\pm 5$ kDyne from the mean force, and $<\pm 100$ μm from the mean tissue displacement were included as part of the experiment. Based on these criteria, a total of 6 animals from the pharmacological cohorts ($n=2$ WT + vehicle [Veh]; $n=1$ WT +0.3 mg/kg of PMX205; $n=1$ WT +1 mg of PMX205; $n=1$ *C5ar2*$^{-/-}$ + Veh; and $n=1$ *C5ar2*$^{-/-}$ + 3 mg/kg of PMX205) and 3 animals from the flow cytometry cohort ($n=1$ WT 2 h post-injury; $n=1$ WT 1 day post-injury; and $n=1$ *C5ar2*$^{-/-}$ 1 day post-injury [dpi]) were excluded from further analysis because their tissue displacement was outside the set limits. Additionally, 4 mice from the pharmacological cohorts ($n=1$ WT + Veh; $n=1$ WT +0.1 mg/kg of PMX205; $n=1$ WT +0.3 mg/kg of PMX205; and $n=1$ *C5ar2*$^{-/-}$ + Veh); 2 mice from the cytokine array cohort ($n=2$ *C5ar2*$^{-/-}$) were excluded because of surgical complications and 1 vehicle-treated *C5ar2*$^{-/-}$ animal died from unidentified causes at 4 days post-SCI. For the remaining animals, there were no significant differences in force or displacement values between experimental groups ($p>0.15$).

Assessment of locomotor function

Functional recovery of hindlimb locomotion was assessed using the 10-point Basso Mouse Scale (BMS), a system designed specifically for the assessment of murine locomotor recovery post-SCI,[32] including ankle movement, stepping, coordination, paw placement, trunk stability, and tail position. Experimental animals were assessed by two investigators blinded to the experimental conditions and/or genotypes at 1, 4, 7, 14, 21, 28, and 35 dpi.

Ex vivo *magnetic resonance imaging*

Experimental mice were sacrificed at 35 dpi. In brief, mice were deeply anesthetized using sodium pentobarbital and then transcardially perfused with 15 mL of saline (0.9% NaCl containing 2 IU/mL of heparin [Pfizer, New York, NY] and 2% $NaNO_2$), followed by 30 mL of phosphate-buffered Zamboni's fixative (2% picric acid and 2% formaldehyde; pH, 7.2–7.4), after which the perfused vertebral columns were excised and post-fixed overnight at 4°C. For imaging purposes, spinal cord samples (cohort 1 only) were washed extensively in 0.1 M of phosphate-buffered saline (PBS). Spinal cords were then immersed in PBS containing gadolinium contrast agent (0.2% Magnevist; Bayer HealthCare Pharmaceuticals, Whippany, NJ) for 48 hours. Vertebral columns containing the spinal cord were imaged using 16.4 Tesla small animal magnetic resonance imaging (MRI; Bruker BioSpin, Billerica, MA), as described previously.[33] Two hundred fifty-six two-dimensional (2D) T2 slices were generated per specimen, with data sets analysed using AVIZO software (version 6.2; Visualization Sciences Group, Burlington, MA); an ortho-slice was set along the sagittal plane and two user-defined (oblique) slices along the coronal and transverse planes, respectively. These axes were set as the reference points for further analyses using the Apply-Transform function. The lasso tool was utilized to create a three-dimensional (3D) reconstruction of the lesion core by manually outlining the hypointense core in the coronal plane of every slice. Confirmation of accurate lesion reconstruction was achieved by viewing the sagittal and transverse planes of the slice. As it can be difficult to differentiate areas of demyelination from remnants of spared gray matter, only the hypointense lesion core was outlined for further analysis and calculation. All aspects of image acquisition and analysis were performed with investigator blinding.

Cytokine analysis and flow cytometry

For cytokine measurements, additional cohorts of WT ($n=8$) and *C5ar2*$^{-/-}$ ($n=8$) mice were subjected to SCI, as detailed earlier, with plasma and spinal cord samples collected at 12 h post-injury; $n=2$ *C5ar2*$^{-/-}$ mice did not recover from surgery/anesthesia and were thus excluded from the study (see Supplementary Table 2 for details) (see online supplementary material at http://www.liebertpub.com). Blood was collected by a left ventricle cardiac puncture using a syringe loaded with 50 μL of 100 mM of ethylenediaminetetraacetic acid (EDTA; Sigma-Aldrich, St. Louis, MO). Next, 10 μL of FUT175 (5 mg/mL; BD Pharmingen, San Diego, CA) were immediately added to the blood sample to prevent complement activation. Samples were then centrifuged for 10 min at 16,900 rcf (relative centrifugal force) and 4°C. The resulting supernatant was retrieved and stored in 40-μL aliquots at −80°C.

Spinal cord samples were obtained by first dissecting the vertebral column from each animal. Following the removal of sutures, which made visible the original laminectomy/lesion site, the dorsal arches of the T8 and T10 vertebra were also removed, after which the exposed spinal cord segment was dissected (caudal boundary of T7 and rostral boundary of T11). The sample was snap-frozen in liquid nitrogen. All spinal cord samples were stored at −80°C until further processing. Frozen spinal cord samples were first weighed and then homogenized with a mortar and pestle on dry ice. Homogenized tissue was transferred to a sample dish containing 200 μL of NP-40 lysis buffer (Invitrogen, Carlsbad, CA) with 0.3 M of phenylmethylsulfonyl fluoride (Sigma-Aldrich) in dimethyl sulfoxide (Sigma-Aldrich), 10 μL of FUT175 (5 mg/mL; BD Pharmingen), and 5 μL of protease inhibitor cocktail (Sigma-Aldrich). Samples were thoroughly resuspended in a 1.5-mL centrifuge tube by vortex for 60 sec, incubated on ice for 1 h, and then centrifuged for 30 min at 16,900rcf and 4°C, after which the supernatant was collected and stored at −80°C.

Sample concentrations of IL-6, IL-10, monocyte chemoattractant protein-1 (MCP-1), interferon-gamma (IFN-γ), tumor necrosis factor alpha (TNFα), and IL-12p70 were determined using a Cytometric Bead Array (BD Biosciences) as per the manufacturer's instructions. Chemokine (C-X-C motif) ligand 1 (CXCL1)/keratinocyte-derived chemokine (KC) and IL-1β levels were also assayed using appropriate Flex sets (BD Biosciences). Data were recorded using a BD LSR II Analyzer Flow cytometer and analyzed as per the manufacturer's instructions.

For flow cytometry, bone marrow (BM) and blood samples were collected from naïve controls and additional cohorts of SCI mice (2 h and 1 dpi) to study the impact of SCI on select leukocyte populations for each genotype ($n = 4$–5 per genotype and time point; see Supplementary Table 2 for details) (see online supplementary material at http://www.liebertpub.com). In brief, mice were anesthetized with methoxyfluorane, followed by the sampling of blood by retro-orbital sinus bleed. A 50-μL aliquot of blood was immediately added to and mixed with 150 μL of anticoagulant buffer (4 mM of EDTA; Sigma-Aldrich) in Dulbecco's phosphate-buffered saline (DPBS; pH 7.4), after which samples were stored on ice until further processing. Next, mice were euthanized with an overdose of sodium pentobarbital (150 mg/kg, i.p.; Virbac Laboratories), their femurs excised and placed in a Petri dish containing RPMI 1640 media (Gibco, Grand Island, NY) for BM isolation. BM was flushed from the femurs with 10 mL of RPMI media (5 mL/femur) using a 10-mL Luer Lock syringe (Terumo Corporation, Tokyo, Japan) with an attached 25g needle (BD, Franklin Lakes, NJ) and then passed through a 40-μm Nylon Cell Strainer (Falcon®; BD) into a 50-mL polypropylene conical tube. BM samples were centrifuged for 10 min at 432rcf and 4°C, after which the supernatant was discarded and the pellet resuspended in 5 mL of red blood cell (RBC) lysis buffer (0.85% NH_4Cl [Univar, Redmond, WA] in ddH_2O). Simultaneously, 1 mL of RBC lysis buffer was added to blood samples, followed by gentle inversion of all samples once every minute over a 5-min incubation.

Blood and BM samples were then centrifuged for 5 min at 200rcf (blood) or 432rcf (BM) and 4°C for white blood cell collection. Cell pellets were resuspended in 100 μL of blocking buffer (0.5% bovine serum albumin [BSA] in 2 mM of EDTA in DPBS) and then counted, after which the cell number per volume for each of the samples was adjusted to the lowest tube concentration for both blood and BM. All samples were then centrifuged for 5 min at 200rcf and 4°C, after which the cell pellets were resuspended in 100 μL of filter-sterilized PBS (pH, 7.2–7.4). Blood and BM samples were incubated with Zombie-Violet viability dye (#423114; BioLegend, San Diego, CA) for 20 min at room temperature (RT), as per the manufacturer's instructions. Sample tubes were then centrifuged for 5 min at 200rcf and 4°C, followed by resuspension in 100 μL of blocking buffer. Rat anti-Mouse CD16/32 (#553142; BD Pharmingen) was added to all tubes, followed by a 10-min incubation for Fc receptor blocking. This was then followed by a further 10-min incubation with biotinylated anti-Gr-1 (#553125; BD Pharmingen), Rat anti-Mouse CD11b-PE conjugate (#101208; BioLegend), and Rabbit anti-Mouse CD3E-AF488 conjugate (#557666; BD Pharmingen), either individually (for individual stain controls, see below) or collectively, as required. Next, 1:400 Streptavidin-647 conjugate (#S-21374; Thermo Fisher Scientific, Waltham, MA) was added, where applicable, to visualize Gr-1 staining. A total of 1 mL of flow-blocking buffer was then added to each tube, after which the samples were centrifuged for 5 min at 200rcf and 4°C.

Supernatants were discarded and the cell pellets resuspended in DPBS with 2 mM of EDTA. All antibodies had been titrated for optimal concentrations and were used at 1:200 and 1:100 dilutions for blood and BM tubes, respectively. With each flow cytometry experiment, separate tubes containing ''cells only'' or individual dye/antibody stains were included to control for staining specificity in both blood and BM samples and/or to allow for the removal of spectral overlap between dyes. Flow-Count™ Fluorospheres (Beckman Coulter, Brea, CA) were added to each test sample to allow for accurate calculations of the total population cell counts. Samples were run through a BD LSRII Analyzer Flow cytometer using FACSDiva software (v6.1; BD Biosciences), with *Area*, *Width*, and *Height* parameters enabled for exclusion of doublets during data analysis. Voltages for each laser were optimized on the individual antibody controls before the running of experiment samples. Compensation was applied to remove any spectral overlap, after which appropriate gating strategies were used for the different leukocyte populations.

Pharmacological blockade of C5aR1 in vivo

The selective and potent cyclic peptide C5aR1 antagonist, PMX205, was used to determine a possible link between altered C5aR1 signaling and SCI outcomes in WT and *C5ar2*$^{-/-}$ mice post-SCI. A dose-response curve was first established in WT mice using 0.1, 0.3, 1, and 3 mg/kg of PMX205, with functional recovery (BMS scores) being the primary outcome measure; isotonic vehicle (5% glucose in ddH_2O) was used as a control. To maximize the effect of C5aR1 antagonism, treatment was initiated 12 h pre-surgery and then maintained with twice-daily administration of PMX205 (12-h intervals) continuing up to 7 dpi. Based on the dose-response relationship for PMX205 in SCI, administration of 3 mg/kg of PMX205 was used in follow-up experiments in which SCI outcomes for WT and *C5ar2*$^{-/-}$ mice were assessed in the presence and absence of (sub-)acute C5aR1 antagonism.

Tissue processing, staining, and analysis

Perfusion-fixed spinal cords were dissected and placed in sequential overnight incubations of 10% and 30% sucrose in PBS for cryoprotection. Next, spinal cords were embedded in Tissue-Tek Optimal Cooling Temperature (Sakura Finetek USA, Inc., Torrance, CA), snap-frozen on dry-ice cooled isopentane, and stored at −80°C until sectioning. Transverse sections of spinal cord were cut at 20-μm intervals using a Leica Cryostat CM3050-S (Leica Microsystems, Wetzlar, Germany) and collected in 1:5 series on Superfrost Plus slides.

For general assessment of histopathology, immunofluorescent staining was used to quantitatively assess myelin, glial fibrillary acidic protein (GFAP), and fibronectin content in tissue sections located proximally, distally, or at the lesion epicenter. Superfrost Plus slides with transverse spinal cord sections of 35 dpi WT and *C5ar2*$^{-/-}$ mice were thawed for 1 h at RT, washed 3 × 5 min in PBS, and then pre-treated with immunohistochemistry (IHC) blocking buffer (2% BSA and 0.2% Triton X-100) for 1 h at RT in a humidified chamber. Slides were then incubated overnight at 4°C with primary antibody solution (1:800 Chicken anti-Mouse GFAP [#ab4674; Abcam, Cambridge, MA] and 1:200 Rabbit anti-Mouse

fibronectin [#F3648; Sigma-Aldrich] diluted in IHC blocking buffer). The following day, slides underwent three 10-min washes in 1×PBS, followed by incubation for 1 h at RT with a secondary antibody cocktail containing 1:400 Goat anti-Rabbit 488 (#A-11034; Thermo Fisher Scientific), 1:800 Donkey anti-Chicken 647 (#703-606-155; Jackson ImmunoResearch, Laboratories, Inc., West Grove, PA), and 1:150 FluoroMyelin Red (#F34652; Thermo Fisher Scientific). Following a further three 10-min PBS washes, slides were mounted using Fluorescent Mounting Medium (Dako, Carpinteria, CA) containing 1:1000 Hoechst nuclear dye (#H3570; Thermo Fisher Scientific). Images were captured on a single plane using a Zeiss Axio Imager at 20× magnification and Zen Blue 2012 Software (Carl Zeiss, Jena, Germany). ImageJ analysis software (National Institutes of Health, Bethesda, MD) was utilized to analyze both the total section area and the respective areas covered by myelin, GFAP, and fibronectin staining. In brief, the section area was determined by outlining the section boundary on the $GFAP^+$ channel (sans meninges) using the Polygon tool. Following this, $FluoroMyelin^+$, $GFAP^+$, or $fibronectin^+$ area was quantified through conversion of images to eight-bit grayscale and analyzed using the Threshold tool. The proportional area measurement of positive staining/total section area percentage was calculated and plotted as the percentage $GFAP^+$ or $Myelin^+$ staining for the section. Approximate 3D-lesion volumes were calculated by multiplying the 2D-area measurement of $fibronectin^+$ tissue by the section thickness (20 μm = 0.02 mm) and series count (5). Lesion volumes were normalized against the total spinal cord volume (TCV) of the analyzed segment to rule out possible size differences between genotypes as a confounding factor. For lesion length, the number of sections with intraparenchymal fibronectin staining was multiplied by the section interval distance (100 μm = 0.1 mm). A total of 4 animals ($n = 1$ WT + Veh; $n = 1$ WT +0.1 mg/kg of PMX205; $n = 1$ WT +3 mg/kg of PMX205; and $n = 1$ *C5ar2*$^{-/-}$ + Veh) were excluded from the histological analysis because of technical issues relating to sectioning.

For quantitative assessment of neutrophil presence at the lesion site, WT and *C5ar2*$^{-/-}$ animals subjected to SCI and then transcardially perfused at 1 dpi with 4% paraformaldehyde, as described previously. Serial spinal cord sections were washed in 1×PBS (3×5 min), followed by incubation in quenching solution 1 (10% MeOH in PBS) for 10 min at RT. Slides were then incubated with quenching solution 2 (10% MeOH with 2% H_2O_2 in PBS) for 20 min at RT. Following this, slides were washed again in PBS and incubated with IHC blocking buffer for 1 h at RT in a humidified chamber. Slides were then incubated overnight at 4°C with Rat anti-Mouse Ly6B.2 (1:400; Bio-Rad Laboratories, Inc., Hercules, CA) in IHC blocking buffer. The following day, slides were washed three times for 10 min in 1×PBS and then incubated for 90 min at RT with 1:200 biotinylated Donkey anti-Rat IgG (#643008; Bio-Rad Laboratories). After another round of washings, slides were incubated for 1 h at RT with VectaStain Elite ABC reagent (1:200 Reagent A and 1:200 Reagent B; Vector Laboratories, Inc., Burlingame, CA). Slides then underwent a further three 10-min washes in 1×PBS, after which the staining was developed with SigmaFAST DAB Peroxidase solution (Sigma-Aldrich) as per the manufacturer's instructions. After ~1 min, slides were immersed in PBS to halt the staining reaction, and then dehydrated by sequential 2-min submersion in 70% ethanol (EtOH; twice), 80% EtOH (once), 90% EtOH (once), and 100% EtOH (twice). Next, slides were immersed in 100% Xylene (twice), mounted (Depex Mounting Medium; Merck & Co., Kenilworth, NJ), and coverslipped. Image-Pro (v6.3; Media Cybernetics, Inc., Rockville, MD) was used to quantify $Ly6B.2^+$ cell numbers at the lesion epicenter.

Statistical analysis

GraphPad Prism (GraphPad Software Inc., La Jolla, CA) was used for data visualization and statistical analysis. Two-way analysis of variance (ANOVA) with Bonferroni's post-hoc test was utilized to analyse *in vivo* BMS data and mobilized leukocyte numbers. One-way ANOVA with Bonferroni's post-hoc test was used to compare 35-dpi BMS scores and myelin sparing in WT animals subjected to either vehicle or different doses of PMX205. For comparisons between two groups (genotypes) or conditions (vehicle vs. drug treatment)—cytokine concentrations and Ly6B.2 staining (1 dpi), BMS scores, and histological data (myelin sparing, $fibronectin^+$ tissue, and GFAP reactivity; 35 dpi)—unpaired two-tailed Student's *t*-tests with Welch's correction and/or two-way ANOVA with least significant difference (LSD) post-hoc were used, as appropriate. Values are presented as experimental group means (± standard error of the mean), with significance achieved at $p < 0.05$ and a statistical power of 0.8 (or greater), unless specified otherwise.

Results

Loss of C5aR2 worsens the outcome from spinal cord injury

Recovery of hindlimb locomotion function was assessed using the 10-point BMS[32] at regular intervals up to 5 weeks post-SCI. All mice displayed normal locomotor function pre-SCI, irrespective of their genotypes, achieving a BMS score of 9. Induction of SCI resulted in near-total hindlimb paralysis in all mice at 1 dpi, after which gradual recovery of hindlimb function was observed in most animals to a final level of at least plantar placement of the paw (BMS score, ≥3). Retrospective analysis of BMS data revealed a consistent trend toward worsened recovery of locomotor function in *C5ar2*$^{-/-}$ mice, which became apparent as early as 4 days post-SCI. *C5ar2*$^{-/-}$ mice regained significantly less hindlimb locomotor function at 14 days post-SCI ($p < 0.01$), and this difference to injured WT controls remained up until the experimental endpoint (35 days post-SCI; Fig. 1A,B). Postmortem analysis provided further evidence of worsened SCI outcomes in the absence of C5aR2, with e*x vivo* MRI revealing significantly larger lesion core volumes in a random sample of *C5ar2*$^{-/-}$ animals ($p < 0.01$; Fig. 1C).

C5aR2 deficiency lowers tumor necrosis factor alpha and interleukin-6 during the acute phase of spinal cord injury

Having established that the absence of C5aR2 negatively impacts on recovery from SCI, we next assessed injury-induced changes in cytokine expression at 12 h post-injury; this time point coincides with clear elevation and/or increased synthesis of cytokines in response to SCI[34] and also complement system activation.[3] Of the various cytokines analyzed, only TNFα and IL-6 levels were differentially regulated between genotypes in response to SCI, with significant reductions observed within spinal cord samples of *C5ar2*$^{-/-}$ mice compared to WT controls ($p < 0.05$; statistical power for IL-6: 0.6; Fig. 2A,B). No significant differences were observed for IFN-γ, MCP-1, IL-1β, KC/CXCL1, or IL-10 ($p > 0.05$; Fig. 2C–G). Additional analysis of plasma samples from injured WT and *C5ar2*$^{-/-}$ mice also revealed no significant differences for any of the aforementioned cytokines between genotypes at the level of the peripheral blood circulation (Fig. 2I–M). IL-12p70 levels were below detection threshold in a significant proportion of spinal cord samples (data not shown), but a significant reduction in plasma levels was observed for this cytokine in *C5ar2*$^{-/-}$ mice (Fig. 2H; $p < 0.05$).

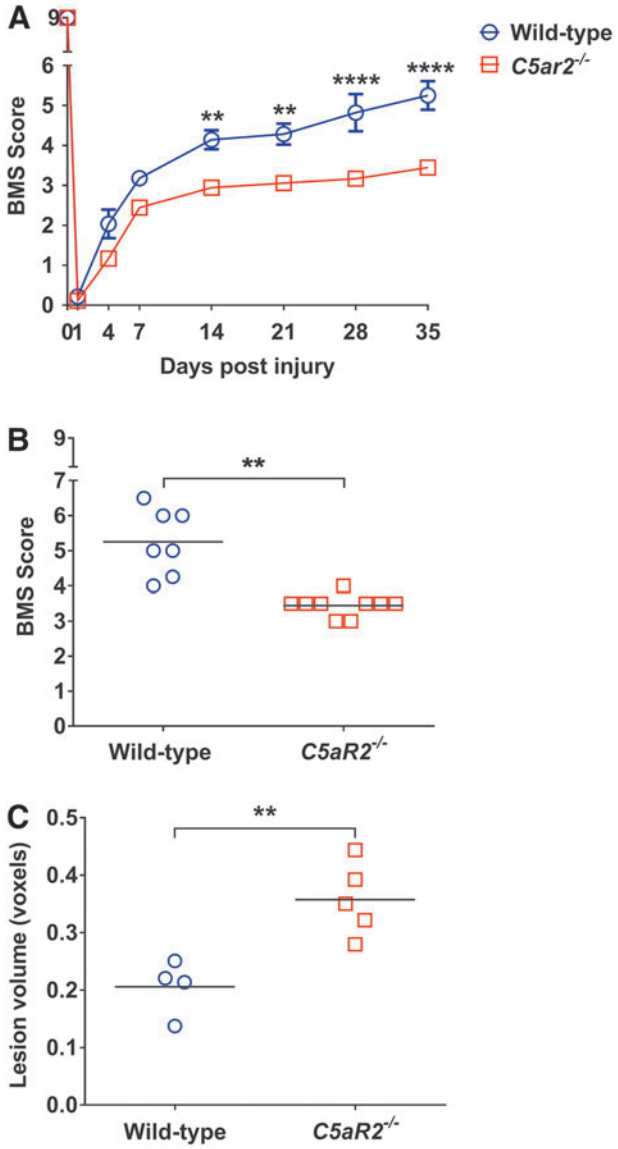

FIG. 1. *C5ar2*$^{-/-}$ mice exhibit worsened recovery from SCI. (**A**) Time course of functional recovery (BMS scores) for WT and *C5ar2*$^{-/-}$ mice. Note that *C5ar2*$^{-/-}$ mice recover significantly less hindlimb locomotor function from 14 dpi onward compared to their age-matched WT counterparts (two-way ANOVA with Bonferroni's; $n=7$ WT, $n=9$ *C5ar2*$^{-/-}$); merged data from two independent experimental repeats. (**B**) Scatter plot showing the group means and individual BMS scores for WT and *C5ar2*$^{-/-}$ mice at the study endpoint (35 dpi; unpaired *t*-test with Welch's correction). (**C**) MRI analysis of lesion core volumes. Note that *C5ar2*$^{-/-}$ mice exhibit larger lesion volumes than their WT counterparts at 35 dpi (unpaired two-tailed Student's *t*-test with Welch's correction). $^{**}p<0.01$; $^{****}p<0.0001$. ANOVA, analysis of variance; BMS, Basso Mouse Scale; dpi, days post-injury; MRI, magnetic resonance imaging; SCI, spinal cord injury; WT, wild type.

Loss of C5aR2 does not impact neutrophil recruitment and/or mobilization of bone marrow leukocytes in acute spinal cord injury

We next explored whether the worsened outcome from SCI for *C5ar2*$^{-/-}$ mice was associated with increased mobilization and recruitment of leukocytes, in particular, neutrophils. Quantification of Ly6B.2^{+} cell numbers at the lesion epicenter at 1 dpi (which is within the peak period of neutrophil recruitment) did not reveal any differences between genotypes (WT, 314 ± 24 cells/mm^2 [$n=4$] vs. *C5ar2*$^{-/-}$: 375 ± 37 cells/mm^2 [$n=5$]; $p=0.22$). Additional flow cytometric analysis of defined white blood cell populations in the blood and BM compartments also did not reveal any differences between genotypes, either under homeostatic (i.e., naïve) or post-injury (2 and 24 h post-SCI; $n=4$–5 per genotype and condition/time point), for neutrophils (CD11b^{+}Gr1^{+}SSC^{hi} cells; $p\geq0.97$), inflammatory monocytes/macrophages (CD11b^{+}Gr1^{+}SSC^{lo} cells; $p\geq0.21$), noninflammatory or patrolling monocytes/macrophages (CD11b^{+}Gr1$^{-/lo}$SSC^{lo} cells; $p\geq0.53$), or T lymphocytes (CD3^{+}SSC^{lo} cells; $p\geq0.48$).

C5aR1 antagonism rescues C5ar2$^{-/-}$ *mice from worsened spinal cord injury recovery*

Although we did not observe overt signs of increased leukocyte mobilization and/or recruitment in absence of C5aR2, these findings still leave open the possibility that the worsened recovery of *C5ar2*$^{-/-}$ mice may have resulted from deregulated C5aR1 signaling given that the influence of C5aR1 over SCI outcomes is conveyed by CNS-resident, not infiltrating, cells.[3] To explore this further, we first established the optimal dose at which the specific C5aR1 antagonist, PMX205, maximally improves SCI outcomes (Fig. 3A). To allow for the maximally possible effect size, treatment was initiated 12 h pre-injury and with a maintenance dosing regimen of twice-daily injections (12 h apart) during the (sub-)acute phase (up to 7 days post-SCI). Based on the primary outcome measure (i.e., BMS scores), low-dose PMX205 treatment (0.1–0.3 mg/kg body weight) was not effective in improving SCI outcomes. In contrast, PMX205 treatment at a dose of either 1 or 3 mg/kg body weight significantly improved recovery of hindlimb locomotor function compared to vehicle-treated controls ($p<0.05$; Fig. 3A). In particular, 5 of 9 (60%) and 8 of 11 (73%) mice treated with 1 or 3 mg/kg of PMX205, respectively, received BMS scores of 5 or higher (frequent to consistent plantar stepping) compared to only 1 of 10 (10%) for vehicle-treated controls.

In direct agreement with the functional outcome, post-mortem analysis of myelin content at the lesion epicenter (secondary endpoint) revealed significant increases in a randomly selected sample of mice that were treated with either 1 or 3 mg/kg of PMX205 compared to vehicle controls (Fig. 3B; $p<0.05$ and $p<0.01$, respectively). Because we previously reported that prolonged loss/inhibition of C5aR1 signaling inhibits astroglial responses to SCI,[3] we also (re-)confirmed that high-dose PMX205 treatment (1 or 3 mg/kg body weight) during the subacute phase of SCI did not have a long-term impact on GFAP immunoreactivity at the lesion

FIG. 2. Comparative analysis of cytokine expression between WT and *C5ar2*$^{-/-}$ mice acutely post-SCI (12 h). Note the significant reductions in intraparenchymal TNF (**A**) and IL-6 (**B**) in spinal cord of *C5ar2*$^{-/-}$ mice compared to injured WT controls. Other cytokines, that is, IFN-γ (**C**), MCP-1 (**D**), IL-1β (**E**), CXCL1 (**F**), or IL-10 (**G**) were not differentially regulated between genotypes. Blood plasma analysis showed that *C5ar2*$^{-/-}$ mice also had significantly lower circulating IL12p70 levels (**H**), but not TNF (**I**), IL-6 (**J**), IFN-γ (**K**), MCP-1 (**L**), and IL-10 (**M**). Unpaired two-tailed Student's *t*-test with Welch's correction; $^{*}p<0.05$. CXCL1, chemokine (C-X-C motif) ligand 1; IFN-γ, interferon-gamma; IL, interlukin; MCP-1, monocyte chemoattractant protein-1; ns, not significant; SCI, spinal cord injury; TNF, tumor necrosis factor; WT, wild type.

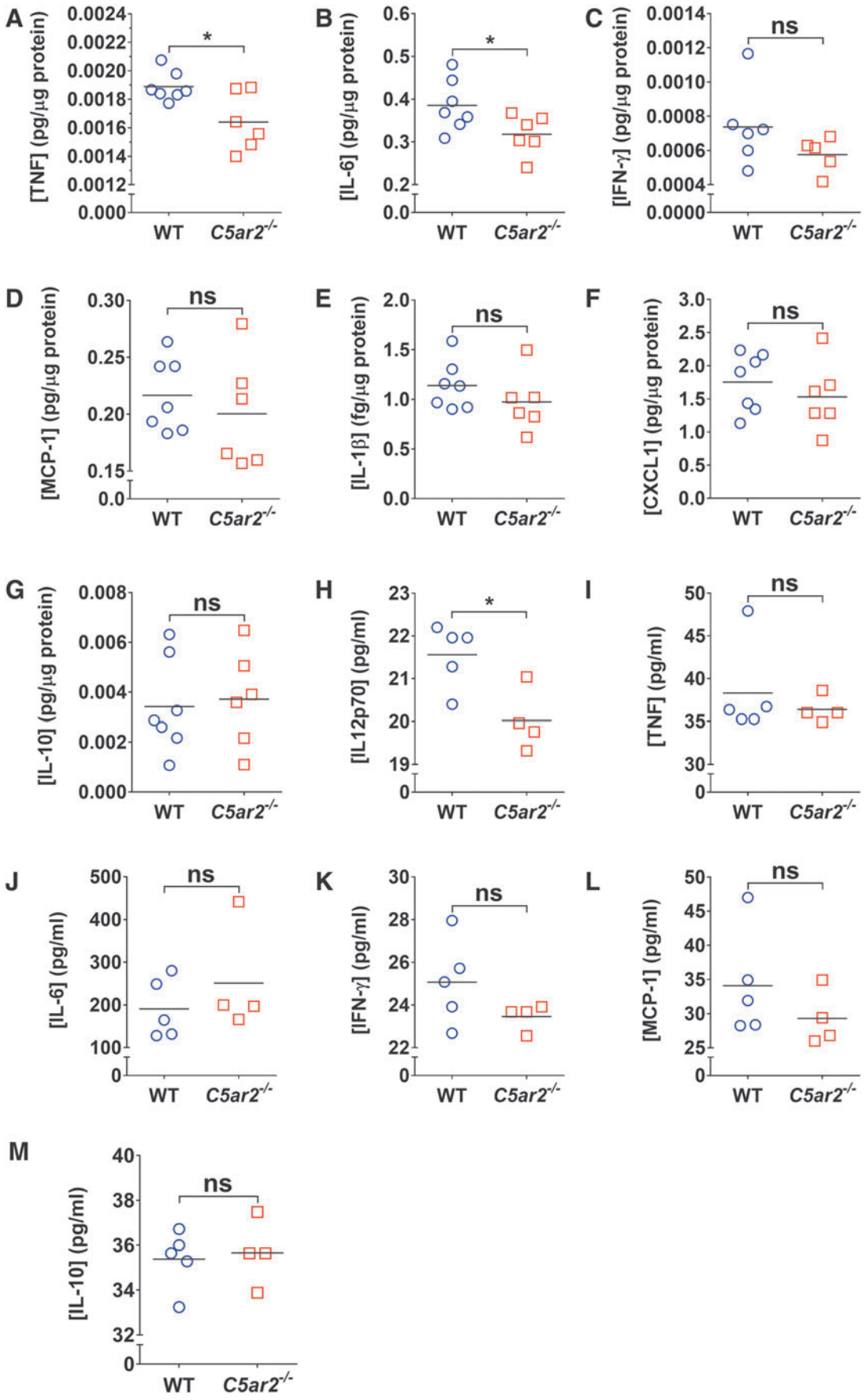
A
[TNF] (pg/μg protein)
0.0024
0.0022
0.0020
0.0018
0.0016
0.0014
0.0012
0.000
*
WT
C5ar2-/-
B
[IL-6] (pg/μg protein)
0.6
0.5
0.4
0.3
0.2
0.0
*
WT
C5ar2-/-
C
[IFN-γ] (pg/μg protein)
0.0014
0.0012
0.0010
0.0008
0.0006
0.0004
0.0000
ns
WT
C5ar2-/-
D
[MCP-1] (pg/μg protein)
0.30
0.25
0.20
0.15
0.0
ns
WT
C5ar2-/-
E
[IL-1β] (fg/μg protein)
2.0
1.5
1.0
0.5
0.0
ns
WT
C5ar2-/-
F
[CXCL1] (pg/μg protein)
3.0
2.5
2.0
1.5
1.0
0.5
0.0
ns
WT
C5ar2-/-
G
[IL-10] (pg/μg protein)
0.008
0.006
0.004
0.002
0.000
ns
WT
C5ar2-/-
H
[IL12p70] (pg/ml)
23
22
21
20
19
0
*
WT
C5ar2-/-
I
[TNF] (pg/ml)
50
45
40
35
30
0
ns
WT
C5ar2-/-
J
[IL-6] (pg/ml)
500
400
300
200
100
0
ns
WT
C5ar2-/-
K
[IFN-γ] (pg/ml)
30
28
26
24
22
0
ns
WT
C5ar2-/-
L
[MCP-1] (pg/ml)
50
45
40
35
30
25
0
ns
WT
C5ar2-/-
M
[IL-10] (pg/ml)
40
38
36
34
32
0
ns
WT
C5ar2-/-

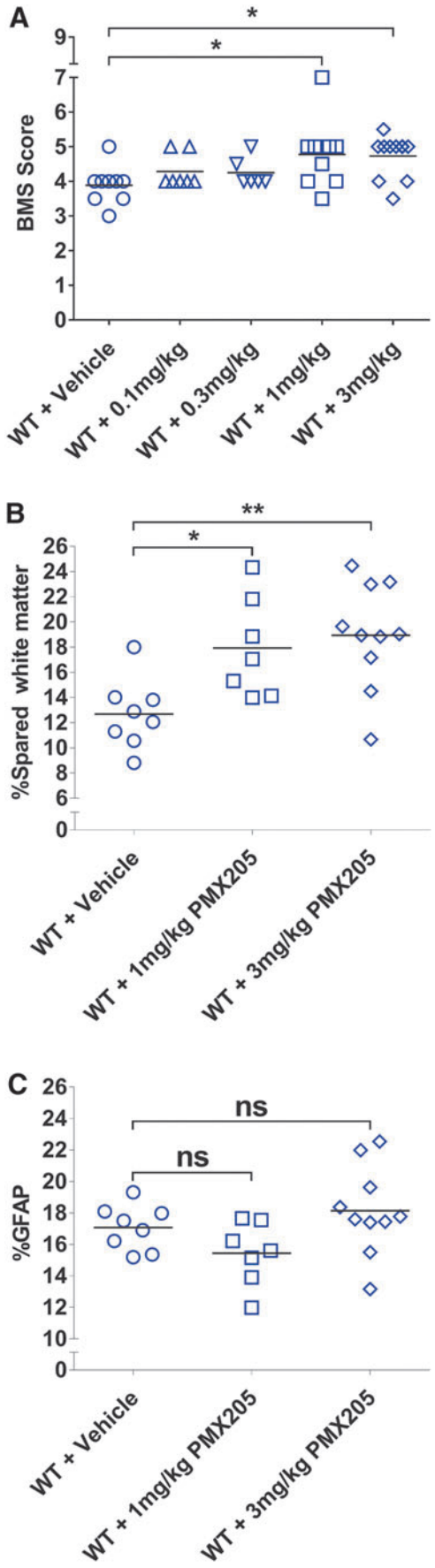

epicenter (Fig. 3C). Based on these results, a dose of 3 mg/kg of PMX205 was chosen for all subsequent experiments.

To directly assess whether C5aR1 antagonism could alleviate, at least in part, the worsened outcome from SCI in the absence of C5aR2, additional cohorts of WT and *C5ar2*$^{-/-}$ mice were subjected to SCI and treated with either vehicle or 3 mg/kg of PMX205 as detailed earlier. As for noninjected animals (Fig. 1), vehicle-treated *C5ar2*$^{-/-}$ mice once again displayed a significantly worsened recovery from SCI compared to their WT counterparts (Fig. 4C; $p < 0.01$). Administration of 3 mg/kg of PMX205 during the (sub-)acute phase of injury significantly improved the functional outcome in both WT and *C5ar2*$^{-/-}$ mice (Fig. 4C; $p < 0.01$). Most important, however, such C5aR1 antagonism reversed the detrimental consequences that resulted from the loss of C5aR2 in relation to SCI recovery, with PMX205-treated *C5ar2*$^{-/-}$ mice now phenocopying their drug-treated WT counterparts ($p = 0.2685$). The benefits of PMX205 treatment in relation to SCI outcomes and for alleviating the worsened recovery of *C5ar2*$^{-/-}$ mice were also evident from post-mortem histological analysis (Fig. 5). Specifically, C5aR1 antagonism (0–7 days post-SCI) significantly and equally improved myelin content at the lesion epicenter in both WT ($p < 0.01$) and *C5ar2*$^{-/-}$ mice ($p < 0.05$) compared to their respective vehicle-treated controls (Fig. 5B). GFAP reactivity at the lesion epicenter was significantly increased in vehicle-treated *C5ar2*$^{-/-}$ mice compared to their WT counterparts ($p < 0.01$); PMX205 treatment attenuated this change (Fig. 5C). Estimation of lesion core volumes based on fibronectin staining revealed a statistically significant effect of PMX205 treatment in *C5ar2*$^{-/-}$, but not WT mice (Fig. 5D); spinal cord volumes were not significantly different between groups ($p > 0.29$). Spatial analysis across the injured spinal cord segment (±1 mm in either rostral and caudal direction) did, however, show a significant treatment overall effect in both genotypes ($F_{3,493} = 19.25$; $p < 0.0001$). Specifically, significant reductions in the fibronectin-positive area (proportional area measurement) were observed in WT mice post-PMX205 treatment between 100 and 300 μm rostral, and for 100 to 200 μm caudal, to the lesion epicenter ($p < 0.05$) compared to their vehicle-treated counterparts. A similar effect of drug treatment was observed in *C5ar2*$^{-/-}$ mice between 200 and 400 μm caudal to the lesion epicenter ($p < 0.05$). Collectively, these findings indicate that the greatest impact of PMX205 treatment in relation to functional recovery appears to be its effect on white matter integrity, as opposed to reducing lesion volume.

Discussion

Activation of the complement cascade post-CNS injury has traditionally been seen as a contributing factor to secondary injury and thus as detrimental to recovery. The primary receptor for C5a,

FIG. 3. Dose-response relationship for C5aR1 antagonism and SCI outcomes. (**A**) Note the significant improvement in functional recovery (BMS scores) for WT animals administered 1 or 3 mg/kg body weight of the selective C5aR1 antagonist, PMX205, during the (sub-)acute phase; doses below 1 mg/kg had no effect on outcomes. (**B**) Higher-dose PMX205 administration (1 and 3 mg/kg body weight) also significantly improved myelin sparing at the lesion epicenter. (**C**) GFAP reactivity at the lesion epicenter was not affected by PMX205 treatment. One-way ANOVA with Bonferroni's; $*p < 0.05$; $**p < 0.01$. ANOVA, analysis of variance; BMS, Basso Mouse Scale; GFAP, glial fibrillary acidic protein; ns, not significant; WT, wild type.

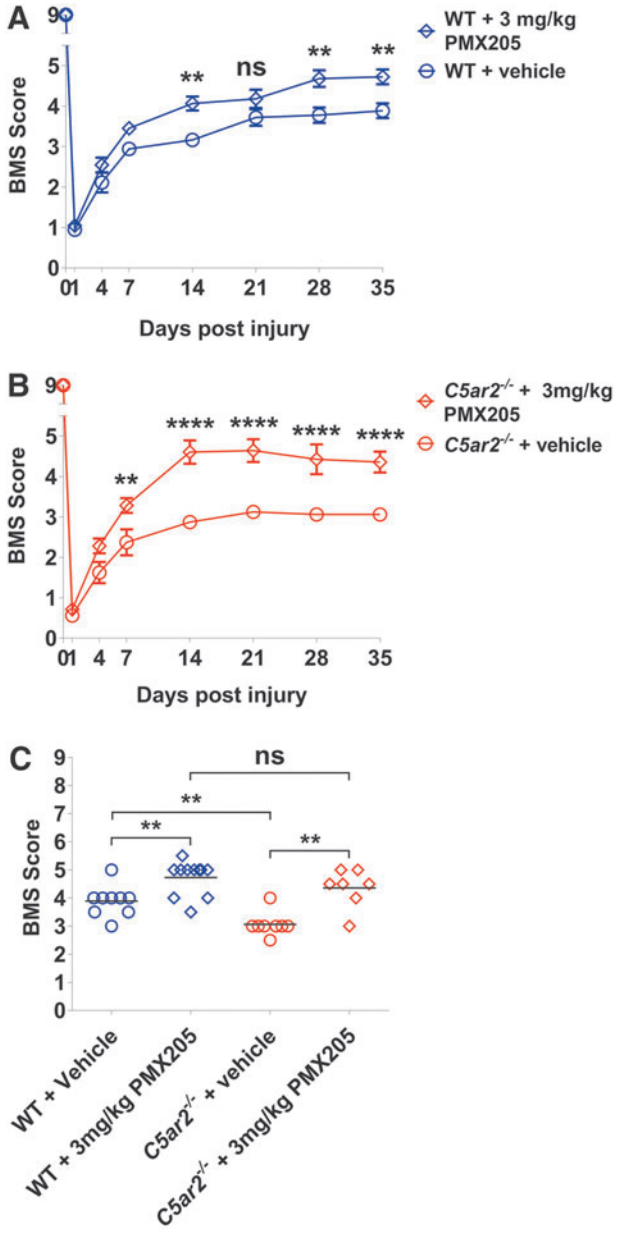

FIG. 4. PMX205 antagonism improves the functional outcomes from SCI and alleviates the *C5ar2*$^{-/-}$ phenotype. (**A** and **B**) Longitudinal data on functional recovery (BMS scores) of WT and *C5ar2*$^{-/-}$ mice treated with either vehicle (5% [isotonic] glucose) or PMX205 (3 mg/kg body weight; two-way ANOVA with Bonferroni's; $n = 7$–11 per genotype and/or treatment group). Note the significant improvement in hindlimb locomotor function (i.e., higher BMS scores) over time for both genotypes after PMX205 administration. (**C**) Scatter plot showing the group means and individual BMS scores for vehicle- and PMX205-treated WT and *C5ar2*$^{-/-}$ mice at the study endpoint (35 dpi; unpaired two-tailed Student's *t*-test with Welch's correction). $^{**}p < 0.01$; $^{****}p < 0.0001$. ANOVA, analysis of variance; BMS, Basso Mouse Scale; dpi, days post-injury; ns, not significant; SCI, spinal cord injury; WT, wild type.

C5aR1, has been implicated in the pathology of intracerebral hemorrhage, ischemic stroke, TBI, and SCI.[3,16–20] Much less is known, however, about the second C5a receptor, C5aR2, particularly in the context of neurological disease. The present study is the first to directly examine the functional contribution of C5aR2 to the outcome from a major neurotraumatic event (i.e., SCI). We report that absence of C5aR2 in mice significantly worsens recovery after traumatic SCI, and that this adverse outcome could be alleviated by C5aR1 inhibition with the specific antagonist, PMX205.

Loss of C5aR2 has a modest impact on cytokine expression in response to spinal cord injury

Previous studies have reported involvement of C5aR2 in restraining expression of proinflammatory cytokines like TNFα, IL-6, CXCL1, IFN-γ, IL-8 (KC/CXCL1), and/or IL-12p40 in various models of peripheral inflammation, including lipopolysaccharide exposure/peritonitis,[28,35] immune complex-mediated pulmonary injury,[36] asthma,[37] or bacterial exposure.[38] In the context of SCI, however, *C5ar2*$^{-/-}$ mice were found to have significantly lower levels of TNFα and IL-6 within the lesioned segment of the spinal cord relative to their WT counterparts at 12 hours post-SCI, suggesting that there is some dependency on this receptor with regard to injury-induced expression of these proinflammatory cytokines; this finding is somewhat consistent with the previously proposed proinflammatory role of C5aR2 in peripheral sepsis,[39] although it should be noted that we did not observe any differences in, for example, IL-6 at the level of the blood. Intraparenchymal expression of other cytokines (i.e., KC/CXCL1, IL-1β, MCP-1, IL-10, and IFN-γ) was unaffected by the loss of C5aR2 in SCI mice. Although previous studies have demonstrated the injurious nature of TNFα and IL-6 signaling during the acute phase of SCI,[40–44] the observed reductions in TNFα and IL-6 in *C5ar2*$^{-/-}$ mice did not confer neuroprotection, at least not on a net basis, given that the loss of C5aR2 in *C5ar2*$^{-/-}$ mice worsened SCI outcomes.

In the blood, only IL12p70 was differentially expressed between genotypes. Specifically, levels of this bioactive cytokine, which is formed from IL-12p35 and IL-12p40, were significantly lower in *C5ar2*$^{-/-}$ plasma post-SCI. Whether or not this may causally relate to the worsened recovery of *C5ar2*$^{-/-}$ mice remains unclear at present given that IL12p70 levels were below detection threshold in spinal cord homogenates. It is interesting to note, however, that direct administration of IL-12p70 to the spinal cord in a hemisection model reportedly improves SCI outcomes, including myelin preservation at the lesion site.[45]

Loss of C5aR2 does not influence leukocyte mobilization in response to spinal cord injury

Flow cytometric analysis revealed no significant differences in the numbers of select leukocyte populations in the BM or blood between genotypes under both homeostatic (i.e., naïve mice) and injured conditions. Specifically, similar numbers of $CD11b^{+}Gr1^{+}SSC\text{-}A^{hi}$ neutrophils and $CD11b^{+}SSC\text{-}A^{lo}$ monocytes were found in WT and *C5ar2*$^{-/-}$ mice, suggesting normal production of these cells under C5aR2-deficient conditions. These findings also indicate that the loss of C5aR2 does not lead to increased mobilization of BM neutrophils in response to tissue injury, as previously reported for the receptor of the complement activation product, C3a.[46] The lack of a clear impact of C5aR2 deficiency on neutrophil mobilization appears somewhat at odds with studies demonstrating a role for C5aR2 in BM neutrophil chemotaxis/influx[14,36] and also a recent report documenting protection against acute C5a-mediated neutrophil mobilization subsequent to selective C5aR2 activation.[22] This discrepancy may be explained by species differences (human vs. mouse) and/or differential reliance on C5a-mediated mobilization/recruitment of polymorphonuclear leukocytes between injury models. Indeed, our previous findings clearly demonstrated that C5a–C5aR1 signaling is not required for neutrophil

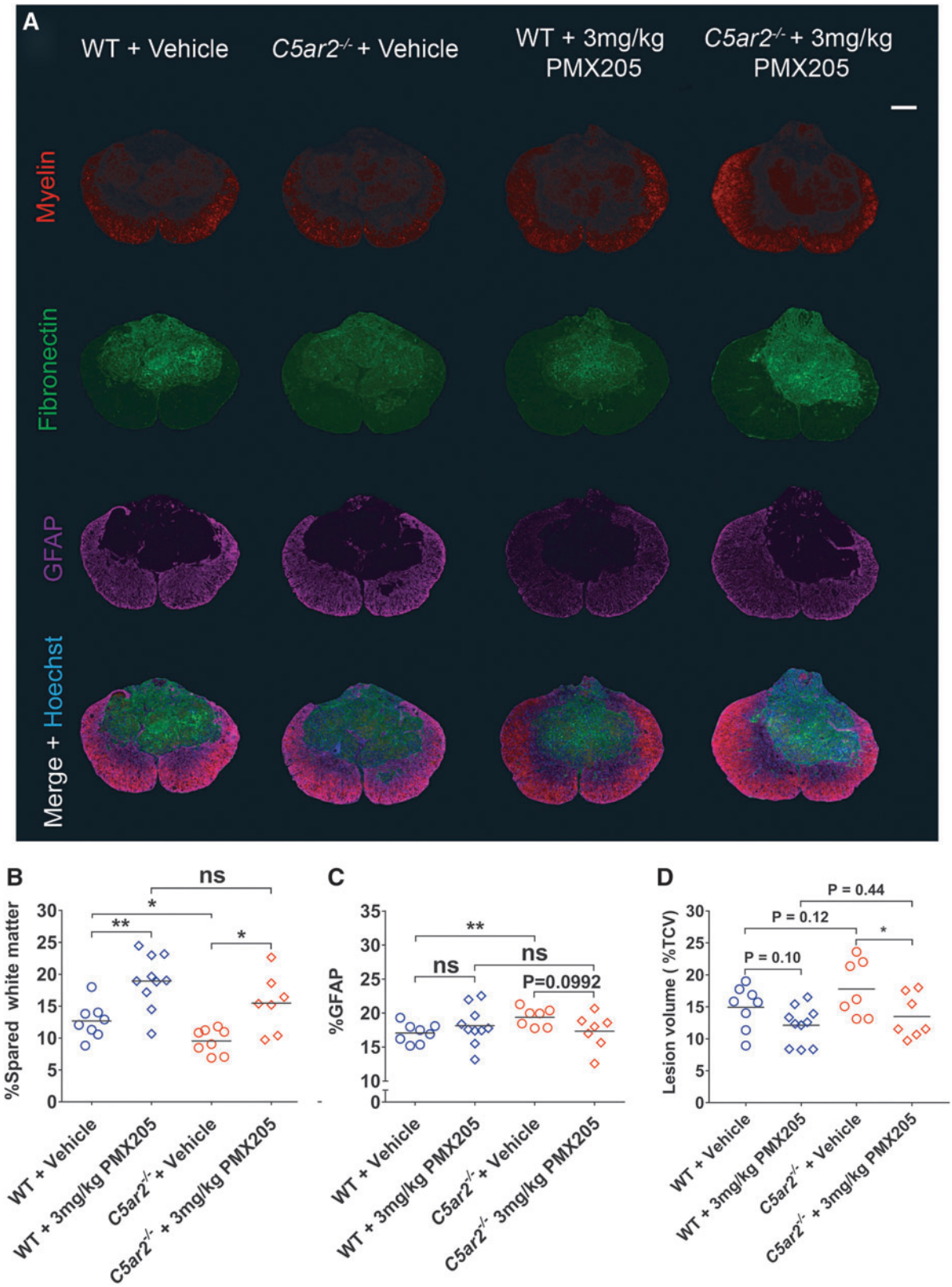

FIG. 5. PMX205 antagonism attenuates SCI histopathology in WT and *C5ar2*$^{-/-}$ mice. (**A**) Representative images of myelin (red), fibronectin (green), and GFAP (magenta) staining at the lesion epicenter for vehicle- and drug-treated WT and *C5ar2*$^{-/-}$ mice. Scale bar (top right): 200 μm. (**B**) Note that PMX205 treatment significantly improved myelin preservation in the ventrolateral white matter of both WT and *C5ar2*$^{-/-}$ mice, also fully reversing the *C5ar2*$^{-/-}$ phenotype. Unpaired two-tailed Student's *t*-test with Welch's correction; $*p < 0.05$; $**p < 0.01$. (**C**) Vehicle-treated *C5ar2*$^{-/-}$ mice displayed increased GFAP immunoreactivity at the lesion epicenter compared to their WT counterparts; this difference was attenuated after PMX205 treatment. Unpaired two-tailed Student's *t*-test with Welch's correction; $**p < 0.01$. (**D**) PMX205 treatment significantly reduced the lesion core volumes in *C5ar2*$^{-/-}$, but not WT, mice. One-way ANOVA with Fisher's LSD post-hoc comparison; $*p < 0.05$. ANOVA, analysis of variance; GFAP, glial fibrillary acidic protein; LSD, least significant difference; ns, not significant; SCI, spinal cord injury; TCV, total cord volume; WT, wild type.

recruitment to the site of SCI in mice[3]; a role for C5aR2 in this process can now also be disregarded.

C5aR2 as a negative regulator of C5aR1 signaling in spinal cord injury?

Although originally considered a nonsignaling decoy receptor,[47] it is now known that C5aR2 can act as a negative regulator of C5aR1 signaling through its interaction with β-arrestin 2[14–22]; C5a-C5aR1 signaling is therefore likely increased in *C5ar2*$^{-/-}$ mice post-SCI. This premise is supported by the observation that administration of the selective C5aR1 antagonist, PMX205,[48] not only improved SCI outcomes, but also counteracted the adverse impact of the loss of C5aR2 on recovery. It is also in agreement with the fact that GFAP immunoreactivity was significantly increased at the lesion epicenter of *C5ar2*$^{-/-}$ mice, because we previously demonstrated that C5a–C5aR1 signaling drives astrocyte proliferation.[3] A limitation of the present study is, however, the fact that we were not able to perform a detailed analysis on the distribution of C5aR2 protein in the injured spinal cord, including what cells coexpress C5aR1 and C5aR2. The lack of a reliable antibody against mouse C5aR2 precluded us from performing such an analysis because all of the available antibodies tested either did not react or showed a similar pattern of staining on *C5ar2*$^{-/-}$ tissue (not shown). Absence of such data does, however, in no way diminish the novelty and significance of our functional studies, which indicate that C5aR2 is neuroprotective and likely influences the outcome from SCI through negative modulation of injurious C5aR1 signaling. Last, one other perceived shortcoming of the present study may be the fact PMX205 treatment was initiated 12 h preceding SCI; we adopted this experimental design to achieve maximal treatment effect for C5aR1 antagonism. Our previous work did, however, already demonstrate that a more clinically relevant approach, that is, post-injury administration of PMX205, also improves SCI outcomes.[3]

Conclusions

The present study confirms the deleterious role of C5a–C5aR1 signaling in acute SCI and also points toward a neuroprotective role for the alternative C5a receptor, C5aR2, in this model of CNS injury. Pharmacological blockade of C5aR1 was able to alleviate the worsened recovery that came with the loss of C5aR2. Early reductions in tissue TNFα and IL-6 in the absence of C5aR2 did not translate into improved outcomes, thereby suggesting that any potential benefit associated with this change in proinflammatory cytokine levels must thus have been outweighed by the loss of neuroprotective mechanisms in *C5ar2*$^{-/-}$ mice. Our findings therefore warrant further investigation into approaches that can either upregulate or selectively activate C5aR2[22] as an alternative strategy for promoting neuroprotection and improving SCI outcomes.

Acknowledgments

This work was supported by the National Health and Medical Research Council of Australia (Project Grant 1060538) and SpinalCure Australia (Career Development Fellowship to M.J.R.). P.J.B. was supported by an Australian Postgraduate Award (The University of Queensland). The authors further thank Mr. Alex Costantini (School of Biomedical Sciences, University of Queensland) for his assistance during the early stages of this project, Mr. Geoff Osbourne and Mrs. Virginia Nink (Queensland Brain Institute, University of Queensland) for help with flow cytometry, Mr. Luke Hammond (Queensland Brain Institute, University of Queensland) for expert assistance with microscopy and image acquisition, and University of Queensland Biological Resources staff for help with animal husbandry.

Author Disclosure Statement

No competing financial interests exist.

References

1. Qiao, F., Atkinson, C., Kindy, M.S., Shunmugavel, A., Morgan, B.P., Song, H., and Tomlinson, S. (2010). The alternative and terminal pathways of complement mediate post-traumatic spinal cord inflammation and injury. Am. J. Pathol. 177, 3061–3070.
2. Anderson, A.J., Robert, S., Huang, W., Young, W., and Cotman, C.W. (2004). Activation of complement pathways after contusion-induced spinal cord injury. J. Neurotrauma 21, 1831–1846.
3. Brennan, F.H., Gordon, R., Lao, H.W., Biggins, P.J., Taylor, S.M., Franklin, R.J., Woodruff, T.M., and Ruitenberg, M.J. (2015). The complement receptor C5aR controls acute inflammation and astrogliosis following spinal cord injury. J. Neurosci. 35, 6517–6531.
4. Dunkelberger, J.R., and Song, W.C. (2010). Complement and its role in innate and adaptive immune responses. Cell Res. 20, 34–50.
5. Manthey, H.D., Woodruff, T.M., Taylor, S.M., and Monk, P.N. (2009). Complement component 5a (C5a). Int. J. Biochem. Cell Biol. 41, 2114–2117.
6. Nataf, S., Stahel, P.F., Davoust, N., and Barnum, S.R. (1999). Complement anaphylatoxin receptors on neurons: new tricks for old receptors? Trends Neurosci. 22, 397–402.
7. Farkas, I., Baranyi, L., Liposits, Z.S., Yamamoto, T., and Okada, H. (1998). Complement C5a anaphylatoxin fragment causes apoptosis in TGW neuroblastoma cells. Neuroscience 86, 903–911.
8. Pavlovski, D., Thundyil, J., Monk, P.N., Wetsel, R.A., Taylor, S.M., and Woodruff, T.M. (2012). Generation of complement component C5a by ischemic neurons promotes neuronal apoptosis. FASEB J. 26, 3680–3690.
9. Leinhase, I., Holers, V.M., Thurman, J.M., Harhausen, D., Schmidt, O.I., Pietzcker, M., Taha, M.E., Rittirsch, D., Huber-Lang, M., Smith, W.R., Ward, P.A., and Stahel, P.F. (2006). Reduced neuronal cell death after experimental brain injury in mice lacking a functional alternative pathway of complement activation. BMC Neurosci. 7, 55.
10. Farkas, I., Takahashi, M., Fukuda, A., Yamamoto, N., Akatsu, H., Baranyi, L., Tateyama, H., Yamamoto, T., Okada, N., and Okada, H. (2003). Complement C5a receptor-mediated signaling may be involved in neurodegeneration in Alzheimer's disease. J. Immunology 170, 5764–5771.
11. Osaka, H., Mukherjee, P., Aisen, P.S., and Pasinetti, G.M. (1999). Complement-derived anaphylatoxin C5a protects against glutamate-mediated neurotoxicity. J. Cell. Biochem. 73, 303–311.
12. Mukherjee, P., and Pasinetti, G.M. (2001). Complement anaphylatoxin C5a neuroprotects through mitogen-activated protein kinase-dependent inhibition of caspase 3. J. Neurochem. 77, 43–49.
13. Mukherjee, P., Thomas, S., and Pasinetti, G.M. (2008). Complement anaphylatoxin C5a neuroprotects through regulation of glutamate receptor subunit 2 in vitro and in vivo. J. Neuroinflammation 5, 5.
14. Bamberg, C.E., Mackay, C.R., Lee, H., Zahra, D., Jackson, J., Lim, Y.S., Whitfeld, P.L., Craig, S., Corsini, E., Lu, B., Gerard, C., and Gerard, N.P. (2010). The C5a receptor (C5aR) C5L2 is a modulator of C5aR-mediated signal transduction. J. Biol. Chem. 285, 7633–7644.
15. Okinaga, S., Slattery, D., Humbles, A., Zsengeller, Z., Morteau, O., Kinrade, M.B., Brodbeck, R.M., Krause, J.E., Choe, H.-R., Gerard, N.P., and Gerard, C. (2003). C5L2, a nonsignaling C5A binding protein. Biochemistry 42, 9406–9415.
16. Li, G., Fan, R.M., Chen, J.L., Wang, C.M., Zeng, Y.C., Han, C., Jiao, S., Xia, X.P., Chen, W., and Yao, S.T. (2014). Neuroprotective effects of argatroban and C5a receptor antagonist (PMX53) following intracerebral haemorrhage. Clin. Exp. Immunol. 175, 285–295.
17. Van Beek, J., Bernaudin, M., Petit, E., Gasque, P., Nouvelot, A., MacKenzie, E.T., and Fontaine, M. (2000). Expression of receptors for complement anaphylatoxins C3a and C5a following permanent focal cerebral ischemia in the mouse. Exp. Neurol. 161, 373–382.
18. Stahel, P.F., Kossmann, T., Morganti-Kossmann, M.C., Hans, V.H., and Barnum, S.R. (1997). Experimental diffuse axonal injury induces enhanced neuronal C5a receptor mRNA expression in rats. Brain Res. Mol. Brain Res. 50, 205–212.

19. Beck, K.D., Nguyen, H.X., Galvan, M.D., Salazar, D.L., Woodruff, T.M., and Anderson, A.J. (2010). Quantitative analysis of cellular inflammation after traumatic spinal cord injury: evidence for a multiphasic inflammatory response in the acute to chronic environment. Brain 133, 433–447.
20. Li, L., Xiong, Z.Y., Qian, Z.M., Zhao, T.Z., Feng, H., Hu, S., Hu, R., Ke, Y., and Lin, J. (2014). Complement C5a is detrimental to histological and functional locomotor recovery after spinal cord injury in mice. Neurobiol. Dis. 66, 74–82.
21. Croker, D.E., Halai, R., Kaeslin, G., Wende, E., Fehlhaber, B., Klos, A., Monk, P.N., and Cooper, M.A. (2014). C5a2 can modulate ERK1/2 signaling in macrophages via heteromer formation with C5a1 and beta-arrestin recruitment. Immunol. Cell Biol. 92, 631–639.
22. Croker, D.E., Monk, P.N., Halai, R., Kaeslin, G., Schofield, Z., Wu, M.C., Clark, R.J., Blaskovich, M.A., Morikis, D., Floudas, C.A., Cooper, M.A., and Woodruff, T.M. (2016). Discovery of functionally selective C5aR2 ligands: novel modulators of C5a signalling. Immunol. Cell Biol. 94, 787–795.
23. Arbore, G., West, E.E., Spolski, R., Robertson, A.A., Klos, A., Rheinheimer, C., Dutow, P., Woodruff, T.M., Yu, Z.X., O'Neill, L.A., Coll, R.C., Sher, A., Leonard, W.J., Kohl, J., Monk, P., Cooper, M.A., Arno, M., Afzali, B., Lachmann, H.J., Cope, A.P., Mayer-Barber, K.D., and Kemper, C. (2016). T helper 1 immunity requires complement-driven NLRP3 inflammasome activity in CD4(+) T cells. Science 352, aad1210.
24. Taoka, Y., Okajima, K., Uchiba, M., Murakami, K., Kushimoto, S., Johno, M., Naruo, M., Okabe, H., and Takatsuki, K. (1997). Role of neutrophils in spinal cord injury in the rat. Neuroscience 79, 1177–1182.
25. Kigerl, K.A., Gensel, J.C., Ankeny, D.P., Alexander, J.K., Donnelly, D.J., and Popovich, P.G. (2009). Identification of two distinct macrophage subsets with divergent effects causing either neurotoxicity or regeneration in the injured mouse spinal cord. J. Neurosci. 29, 13435–13444.
26. Lee, S.M., Rosen, S., Weinstein, P., van Rooijen, N., and Noble-Haeusslein, L.J. (2011). Prevention of both neutrophil and monocyte recruitment promotes recovery after spinal cord injury. J. Neurotrauma 28, 1893–1907.
27. Popovich, P.G., Guan, Z., Wei, P., Huitinga, I., van Rooijen, N., and Stokes, B.T. (1999). Depletion of hematogenous macrophages promotes partial hindlimb recovery and neuroanatomical repair after experimental spinal cord injury. Exp. Neurol. 158, 351–365.
28. Chen, N.J., Mirtsos, C., Suh, D., Lu, Y.C., Lin, W.J., McKerlie, C., Lee, T., Baribault, H., Tian, H., and Yeh, W.C. (2007). C5L2 is critical for the biological activities of the anaphylatoxins C5a and C3a. Nature 446, 203–207.
29. Kilkenny, C., Browne, W.J., Cuthill, I.C., Emerson, M., and Altman, D.G. (2010). Improving bioscience research reporting: the ARRIVE guidelines for reporting animal research. PLoS Biol. 8, e1000412.
30. Scheff, S.W., Rabchevsky, A.G., Fugaccia, I., Main, J.A., and Lumpp, J.E., Jr. (2003). Experimental modeling of spinal cord injury: characterization of a force-defined injury device. J. Neurotrauma 20, 179–193.
31. Harrison, M., O'Brien, A., Adams, L., Cowin, G., Ruitenberg, M.J., Sengul, G., and Watson, C. (2013). Vertebral landmarks for the identification of spinal cord segments in the mouse. Neuroimage 68, 22–29.
32. Basso, D.M., Fisher, L.C., Anderson, A.J., Jakeman, L.B., McTigue, D.M., and Popovich, P.G. (2006). Basso Mouse Scale for locomotion detects differences in recovery after spinal cord injury in five common mouse strains. J. Neurotrauma 23, 635–659.
33. Blomster, L.V., Cowin, G.J., Kurniawan, N.D., and Ruitenberg, M.J. (2013). Detection of endogenous iron deposits in the injured mouse spinal cord through high-resolution ex vivo and in vivo MRI. NMR Biomed. 26, 141–150.
34. Pineau, I., and Lacroix, S. (2007). Proinflammatory cytokine synthesis in the injured mouse spinal cord: multiphasic expression pattern and identification of the cell types involved. J. Comp. Neurol. 500, 267–285.
35. Bachmaier, K., Guzman, E., Kawamura, T., Gao, X., and Malik, A.B. (2012). Sphingosine kinase 1 mediation of expression of the anaphylatoxin receptor C5L2 dampens the inflammatory response to endotoxin. PLoS One 7, e30742.
36. Gerard, N.P., Lu, B., Liu, P., Craig, S., Fujiwara, Y., Okinaga, S., and Gerard, C. (2005). An anti-inflammatory function for the complement anaphylatoxin C5a-binding protein, C5L2. J. Biol. Chem. 280, 39677–39680.
37. Zhang, X., Schmudde, I., Laumonnier, Y., Pandey, M.K., Clark, J.R., Konig, P., Gerard, N.P., Gerard, C., Wills-Karp, M., and Kohl, J. (2010). A critical role for C5L2 in the pathogenesis of experimental allergic asthma. J. Immunol. 185, 6741–6752.
38. Raby, A.C., Holst, B., Davies, J., Colmont, C., Laumonnier, Y., Coles, B., Shah, S., Hall, J., Topley, N., Kohl, J., Morgan, B.P., and Labeta, M.O. (2011). TLR activation enhances C5a-induced pro-inflammatory responses by negatively modulating the second C5a receptor, C5L2. Eur. J. Immunol. 41, 2741–2752.
39. Rittirsch, D., Flierl, M.A., Nadeau, B.A., Day, D.E., Huber-Lang, M., Mackay, C.R., Zetoune, F.S., Gerard, N.P., Cianflone, K., Kohl, J., Gerard, C., Sarma, J.V., and Ward, P.A. (2008). Functional roles for C5a receptors in sepsis. Nat. Med. 14, 551–557.
40. Ferguson, A.R., Christensen, R.N., Gensel, J.C., Miller, B.A., Sun, F., Beattie, E.C., Bresnahan, J.C., and Beattie, M.S. (2008). Cell death after spinal cord injury is exacerbated by rapid TNF alpha-induced trafficking of GluR2-lacking AMPARs to the plasma membrane. J. Neurosci. 28, 11391–11400.
41. Okada, S., Nakamura, M., Mikami, Y., Shimazaki, T., Mihara, M., Ohsugi, Y., Iwamoto, Y., Yoshizaki, K., Kishimoto, T., Toyama, Y., and Okano, H. (2004). Blockade of interleukin-6 receptor suppresses reactive astrogliosis and ameliorates functional recovery in experimental spinal cord injury. J. Neurosci. Res. 76, 265–276.
42. Mukaino, M., Nakamura, M., Yamada, O., Okada, S., Morikawa, S., Renault-Mihara, F., Iwanami, A., Ikegami, T., Ohsugi, Y., Tsuji, O., Katoh, H., Matsuzaki, Y., Toyama, Y., Liu, M., and Okano, H. (2010). Anti-IL-6-receptor antibody promotes repair of spinal cord injury by inducing microglia-dominant inflammation. Exp. Neurol. 224, 403–414.
43. Guerrero, A.R., Uchida, K., Nakajima, H., Watanabe, S., Nakamura, M., Johnson, W.E., and Baba, H. (2012). Blockade of interleukin-6 signaling inhibits the classic pathway and promotes an alternative pathway of macrophage activation after spinal cord injury in mice. J. Neuroinflammation 9, 40.
44. Arima, H., Hanada, M., Hayasaka, T., Masaki, N., Omura, T., Xu, D., Hasegawa, T., Togawa, D., Yamato, Y., Kobayashi, S., Yasuda, T., Matsuyama, Y., and Setou, M. (2014). Blockade of IL-6 signaling by MR16-1 inhibits reduction of docosahexaenoic acid-containing phosphatidylcholine levels in a mouse model of spinal cord injury. Neuroscience 269, 1–10.
45. Yaguchi, M., Ohta, S., Toyama, Y., Kawakami, Y., and Toda, M. (2008). Functional recovery after spinal cord injury in mice through activation of microglia and dendritic cells after IL-12 administration. J. Neurosci. Res. 86, 1972–1980.
46. Wu, M.C., Brennan, F.H., Lynch, J.P., Mantovani, S., Phipps, S., Wetsel, R.A., Ruitenberg, M.J., Taylor, S.M., and Woodruff, T.M. (2013). The receptor for complement component C3a mediates protection from intestinal ischemia-reperfusion injuries by inhibiting neutrophil mobilization. Proc. Natl. Acad. Sci. U. S. A. 110, 9439–9444.
47. Scola, A.M., Johswich, K.O., Morgan, B.P., Klos, A., and Monk, P.N. (2009). The human complement fragment receptor, C5L2, is a recycling decoy receptor. Mol. Immunol. 46, 1149–1162.
48. Woodruff, T.M., Pollitt, S., Proctor, L.M., Stocks, S.Z., Manthey, H.D., Williams, H.M., Mahadevan, I.B., Shiels, I.A., and Taylor, S.M. (2005). Increased potency of a novel complement factor 5a receptor antagonist in a rat model of inflammatory bowel disease. J. Pharmacol. Exp. Ther. 314, 811–817.

Address correspondence to:
Marc J. Ruitenberg, PhD
School of Biomedical Sciences
The University of Queensland
St Lucia, QLD 4072
Australia

E-mail: m.ruitenberg@uq.edu.au